IOP Conf. Series: Journal of Physics: Conf. Series **931** (2017) 012006 doi:10.1088/1742-6596/931/1/012006

Computation of an MRI brain atlas from a population of Parkinson's disease patients

L Angelidakis[1], I E Papageorgiou[2,3], C Damianou[1], M N Psychogios[3], P Lingor[4], K von Eckardstein[5], S Hadjidemetriou[1]

[1]Department of Electrical Engineering and Informatics, Cyprus University of Technology, Limassol, Cyprus

[2]Institute of Diagnostic and Interventional Radiology University of Jena, Jena, Germany

[3]Department of Diagnostic and Interventional Neuroradiology,

[4]Department of Neurology, [5]Department of Neurosurgery, University Medical Center Goettingen, University of Goettingen, Goettingen, Germany

Corresponding Author: Lasthenis Angelidakis, lg.angelidakis@edu.cut.ac.cy

Abstract. Parkinson's Disease (PD) is a degenerative disorder of the brain. This study presents an MRI-based brain atlas of PD to characterize associated alterations for diagnostic and interventional purposes. The atlas standardizes primarily the implicated subcortical regions such as the globus pallidus (GP), substantia nigra (SN), subthalamic nucleus (STN), caudate nucleus (CN), thalamus (TH), putamen (PUT), and red nucleus (RN). The data were 3.0 T MRI brain images from 16 PD patients and 10 matched controls. The images used were T1-weighted (T_1w), T2-weighted (T_2w) images, and Susceptibility Weighted Images (SWI). The T1w images were the reference for the inter-subject non-rigid registration available from 3DSlicer. Anatomic labeling was achieved with BrainSuite and regions were refined with the level sets segmentation of ITK-Snap. The subcortical centers were analyzed for their volume and signal intensity. Comparison with an age-matched control group unravels a significant PD-related T1w signal loss in the striatum (CN and PUT) centers, but approximately a constant volume. The results in this study improve MRI based PD localization and can lead to the development of novel biomarkers.

Keywords: Brain 3 Tesla MRI atlas, SWI, Parkinson´s disease biomarkers, striatum, basal ganglia, 3DSlicer, neurodegeneration.

1. Introduction

Parkinson's disease (PD) is a neurodegenerative disorder that mainly affects the motor system. Magnetic Resonance Imaging (MRI) plays an increasing role as a non-invasive imaging diagnostic tool for neurodegeneration with structural and morphological information. The recent developments of specific sequences such as the Susceptibility-Weighted Imaging (SWI) improves the imaging of midbrain structures significant for PD [1].

The collection and quantification of MRI-datasets enables the assembly of "human brain atlases" as references for spatial normalization and structural segmentation. This can assist not only interventional navigation, but also diagnosis. Many brain atlases are computed from healthy subjects [2,3]. However, general population atlases are typically not representative of the brain degeneration in PD. Thus, recent initiatives promote the construction of disease-specific brain atlases [4].

The aim of this work has been to develop an MRI-based brain atlas representative of PD-brain alterations for interventional and diagnostic purposes. The main goal of the atlas is to localize the implicated subcortical regions, such as the TH, GP, RN, SN, PUT, STN, and CN. This can improve

the focusing of electrode implantation for Deep Brain Stimulation (DBS). Also, the atlas characterizes these anatomic regions in terms of their volumes and signal intensities. The comparison with age-and-gender matched controls can lead to the development of biomarkers for PD.

2. Materials and Methods

The imaging data were from $N = 16$ PD patients of mean age $60 \pm 9\ years$ (11 M, 5 F). The images $(I_i(x), \ldots\ldots, I_N(x))$, where x denotes space, were of three different contrasts, T_1w MPRAGE, T_2w, and SWI. The data was retrieved from the Parkinson's Database of University Medical center Göttingen for acquisitions between 01/2011 and 01/2016. The imaging was performed with a MAGNETOM Trio TIM MR-system 3.0 T (Siemens, Erlangen, Germany) and a dedicated 32-channel head coil. The patients were in total anesthesia. The image analysis was performed with 3DSlicer [5]. The T_1w images were denoised with a median filter. A brain mask, M_i, was delineated manually from the corresponding T_1w image. The registration was first intra-subject to the T_1w image. First, a rigid $T_{R,1}$ with 6 degrees of freedom (dof) and then an affine $T_{R,2}$ of 12 dof. The total intra-subject registration is their concatenation, $(T_{R,1} * T_{R,2})$, where * is convolution. The next step was bias correction with N4ITK [6]. Then, a representative T_1w image was selected as reference, I_{REF} for inter-subject non-rigid registration T_{NR}. The T_{NR} was based on BSplines with $6 \times 6 \times 6 = 216$ nodes. All transformations were also applied to M_i to obtain $M_i(T_{NR} * T_{R,2} * T_{R,1} * x)$. The multiplication with I_i gives $I_i \times M_i(T_{NR} * T_{R,2} * T_{R,1} * x)$ and isolates the brain region. The brain regions histograms of all images were normalized to have the same white matter peak as that of the reference image, I_{Ref}. Normalization was necessary to make the intensity ranges of the tissues distributions comparable. This allows considering them together and computing their average image. The T_1w brain atlas $I_{atl,T1}$ was the average image, $I_{atl,T1} = 1/N \sum_{i=1}^{N-1} I_i(T_{NR} * T_{R,2} * T_{R,1} * x)$. The atlases of the T_2w images, $I_{atl,T2}$, and SWI images, $I_{atl,SWI}$, were computed with the application of the corresponding transformations $(T_{NR} * T_{R,2} * T_{R,1})$ computed from the T_1w images.

To localize the different brain regions of interest we co-registered the $I_{atl,T1}$ to the labeled BCI-DNI brain atlas available through BrainSuite [7]. This atlas provided initialization of the anatomic regions of interest that were the TH, GP, PUT, and CN. These regions were refined with the level-sets segmentation method of ITK-SNAP [8]. Other fine midbrain structures, namely, the RN, SN and STN were manually segmented by the first author with ITK-SNAP. These segmentations were then corrected by two of the co-authors that are qualified physicians I.E.P. and M.N.P., with three and twelve years of experience respectively. The involvement of two different reviewers following the practices of two different medical centers minimizes subjectivity and thus increases reproducibility. All segmented regions were analyzed for volume and intensity.

The control data consisting of $N = 10$ age-gender matched patients of mean age $48 \pm 5\ years$ (4 M, 6 F) without neurodegenerative changes were processed with the same steps as those described above. They produced a T_1w brain atlas $I_{atl,T1}$ as well as the anatomic regions of the TH, GP, PUT, and CN. The information derived from the segmentations of the brain structures for PD and healthy subjects were compared in terms of their volume and their intensities with Student´s 2-tailed t-test or with the non-parametric Mann–Whitney U tests with Sigma Plot™ (Systat Software Inc., San Jose, CA USA). The diagnostic sensitivity (SE) and specificity (SP) of the analyzed parameters were evaluated with Receiver Operating Characteristics (ROC) and the Cut-off values were determined with Youden J statistics.

3. Results

In this study both signal intensity and volume have been selected as MRI correlates for the pathological changes occurring in PD. Neurodegeneration is intuitively associated with loss of

volume, "involution", of the subcortical nuclei. Moreover, depositions of protein inclusions, cell debris and gliosis significantly modify the proton density and variously affect the $\boldsymbol{T_1w/T_2w}$ signal [9].

3.1. MRI-based brain atlases, Volume and Signal Intensity of the basal ganglia as biomarkers

The images from N=16 PD patients and N=10 control provided brain atlases for the PD-brain and for age- and gender-matched controls as shown in 'figure 1'. In contrast to the midbrain tegmentum (SN and RN), the GP, the striatum which is part of basal ganglia, and the TH are well identifiable in the T_1w MPRAGE image from the 16 PD and the 10 control subjects. Based on the segmentations outer contours we generated 3D-surface renderings with 3DSlicer for the striatal area focusing on the CN 'figure 2' (i, ii, iii). Representative axial, sagittal and coronal T_1w images with color-coding of the segmented nuclei (blue) are shown in the panel below the surface renderings in 'figure 2' (iv, v, vi). PD patients were analyzed for volume and T_1w signal intensity changes compared to the control group.

We analyzed the CN whose volume is not significantly affected by PD, P=0.43, 2-tailed t-test in 'figure 2' (b), most of the other analyzed regions followed the same pattern. However, the T_1w signal intensity is significantly reduced in PD patients in 'figure 2' P < 0.0001, 2-tailed t-test (c) by approximately 8% from the average control value. The parameter for the ROC analysis was the T_1w intensity and its diagnostic efficacy is high as shown in 'figure 2' (d), with an $AUC = 0.93 \pm 0.07$. By implementing Youden statistics for the T_1w signal intensity we could reveal a cut-off diagnostic value of 352.5 with a SE of 100% and a SP of 90% for PD versus the control shown in 'figure 2' (c). In summary, even though PD is not associated with striatal involution, it affects the T_1w signal intensity of the caudate nucleus compared to an age- and gender- matched control population. Thus, the ROC analysis suggests that PD-related signal loss in the T_1w sequence is a potential sensitive diagnostic parameter for PD.

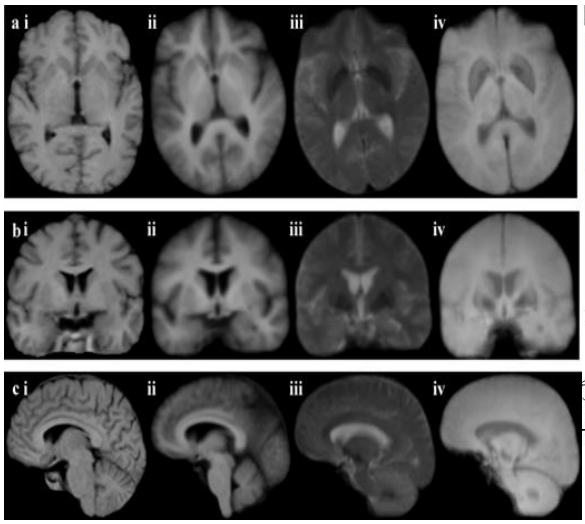

Figure 1 (left). MRI brain atlas. (**I**) Probabilistic average images from population, T_1w, N=10. **(II)** Probabilistic average images from PD patients, T_1w, (**III**) , T_2w PD and (IV) SWI PD, N=16.

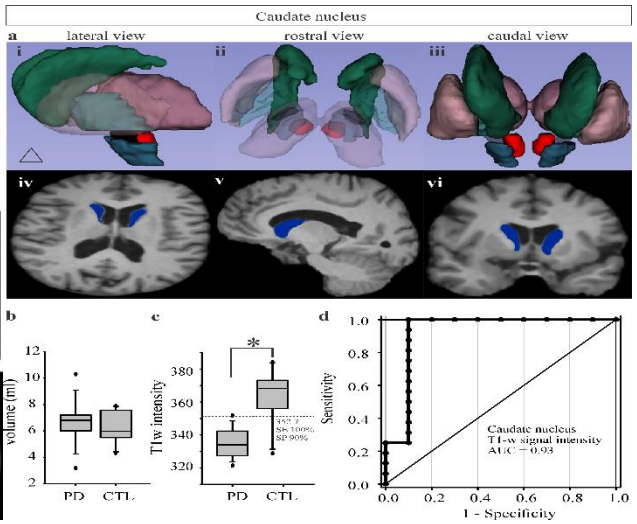

Figure 2 (right). Volume and intensity analysis of the caudate nucleus. Sample PD-brain 3D surface-renderings of the basal ganglia (CN, *dark green*; PUT, *light pink*; GP, *light green*; TH, *dark pink*) and the midbrain nuclei (SN, *marine blue*; RN, *red*) as well as the STN (*black*). (**Aiv**) Axial, (**Av**) sagittal and (**Avi**) coronal T_1w sections with blue-shaded CN. (**B**) Volume analysis of the CN (**C**) Intensity analysis (**D**) ROC of the T_1w MPRAGE intensity of the CN, PD *N*=16, control *N*=10.

4. Discussion

The PD brain atlas and quantification in this study focuses not only on the primarily affected midbrain regions (SN), but also on the downstream affected basal ganglia, especially the striatum. The striatum, receives dopaminergic innervation from the SN, hence undergoing "denervation" secondarily to nigral neurodegeneration [10]. This is associated with neural dystrophy but not necessarily with neuronal death [11]. This is in agreement with our findings, classical radiological descriptions and neuropathology converge toward the opinion that PD is not associated with striatal involution [12]. Apart from the loss of volume, we analyzed the subregions for signal intensity as an imaging correlate of histological remodeling. We showed a significant signal loss of the striatum (CN) in PD compared to controls. Such signal alteration may represent initial structural changes and neuronal loss that do not necessarily reflect volume loss.

The main target of this study was to create an MRI brain atlas of the PD brain based on retrospective data acquisition from an existing database. The platform of the atlas is flexible to modifications and can be enriched with additional subjects. A limitation of this study is that the control database consisted of only T_1w images. Thus, volume and intensity alterations could not be reported for structures defined by the T_2w image and the SWI signal, specifically for the SN and STN.

References

[1] Zhang J, Zhang Y, Wang J, Cai P, Luo C, Qian Z, Dai Y and Feng H 2010 Characterizing iron deposition in Parkinson's disease using susceptibility-weighted imaging: An in vivo MR study Brain Res. **1330** 124–30

[2] Talairach J and Tournoux P 1988 Co-planar stereotaxic atlas of the human brain: 3-dimensional proportional system: an approach to cerebral imaging (Stuttgart ; New York: Georg Thieme)

[3] Rohlfing T, Zahr N M, Sullivan E V and Pfefferbaum A 2008 The SRI24 multichannel brain atlas: construction and applications ed J M Reinhardt and J P W Pluim p 691409

[4] Xiao Y, Fonov V, Bériault S, Al Subaie F, Chakravarty M M, Sadikot A F, Pike G B and Collins D L 2015 Multi-contrast unbiased MRI atlas of a Parkinson's disease population Int. J. Comput. Assist. Radiol. Surg. **10** 329–41

[5] Fedorov A, Beichel R, Kalpathy-Cramer J, Finet J, Fillion-Robin J-C, Pujol S, Bauer C, Jennings D, Fennessy F, Sonka M, Buatti J, Aylward S, Miller J V, Pieper S and Kikinis R 2012 3D Slicer as an image computing platform for the Quantitative Imaging Network Magn. Reson. Imaging **30** 1323–41

[6] Tustison N J, Avants B B, Cook P A, Yuanjie Zheng, Egan A, Yushkevich P A and Gee J C 2010 N4ITK: Improved N3 Bias Correction IEEE Trans. Med. Imaging **29** 1310–20

[7] Shattuck D W and Leahy R M 2002 BrainSuite: an automated cortical surface identification tool Med. Image Anal. **6** 129–42

[8] Yushkevich P A, Piven J, Hazlett H C, Smith R G, Ho S, Gee J C and Gerig G 2006 User-guided 3D active contour segmentation of anatomical structures: significantly improved efficiency and reliability NeuroImage **31** 1116–28

[9] Goubran M, Hammond R R, de Ribaupierre S, Burneo J G, Mirsattari S, Steven D A, Parrent A G, Peters T M and Khan A R 2015 Magnetic resonance imaging and histology correlation in the neocortex in temporal lobe epilepsy Ann. Neurol. **77** 237–50

[10] Hanganu A, Provost J-S and Monchi O 2015 Neuroimaging studies of striatum in cognition part II: Parkinson's disease Front. Syst. Neurosci. **9**

[11] Villalba R M and Smith Y 2010 Striatal Spine Plasticity in Parkinson's Disease Front. Neuroanat. **4**

[12] Dickson D W 2017 Neuropathology of Parkinson disease Parkinsonism Relat. Disord.